Aus dem Zentrum für Augenheilkunde der Universität zu Köln
Klinik und Poliklinik für Allgemeine Augenheilkunde
Direktor: Universitätsprofessor Dr. med. C. Cursiefen

Reproducibility of Three-Dimensional Stereophotogrammetry in Measuring Periocular Tumor Area and Volume

Inaugural-Dissertation zur Erlangung der Doktorwürde
der Medizinischen Fakultät
der Universitätzu Köln

vorgelegtvon
Xincen Hou
aus Shandong, China

promoviert am 16. Juni 2025

Gedruckt mit Genehmigung der Medizinischen Fakultät der Universität zu Köln

Druckjahr: 2025

Dekan: Universitätsprofessor Dr. med. G. R. Fink

1. Gutachter: Universitätsprofessor Dr. med. Dr. phil. L. M. Heindl
2. Gutachterin: Privatdozentin Dr. med. T. Schick

Erklärung

Ich erkläre hiermit, dass ich die vorliegende Dissertationsschrift ohne unzulässige Hilfe Dritter und ohne Benutzung anderer als der angegebenen Hilfsmittel angefertigt habe; die aus fremden Quellen direkt oder indirekt übernommenen Gedanken sind als solche kenntlich gemacht.

Bei der Auswahl und Auswertung des Materials sowie bei der Herstellung des Manuskriptes habe ich Unterstützungsleistungen von folgenden Personen erhalten:

Universitätsprofessor Dr. Dr. Ludwig M. Heindl, Priv.-Doz. Dr. med. Alexander C. Rokohl, Dr. med. Yongwei Guo, Dr. med. Wanlin Fan.

Weitere Personen waren an der Erstellung der vorliegenden Arbeit nicht beteiligt. Insbesondere habe ich nicht die Hilfe einer Promotionsberaterin/eines Promotionsberaters in Anspruch genommen. Dritte haben von mir weder unmittelbar noch mittelbar geldwerte Leistungen für Arbeiten erhalten, die im Zusammenhang mit dem Inhalt der vorgelegten Dissertationsschrift stehen.

Die Dissertationsschrift wurde von mir bisher weder im Inland noch im Ausland in gleicher oder ähnlicher Form einer anderen Prüfungsbehörde vorgelegt.

Die dieser Arbeit zugrunde liegenden Daten wurden durch meine Mitarbeit im Zentrum für Augenheilkunde der Universität zu Köln ermittelt.

Diese Daten wurden von Herrn Universitätsprofessor Dr. med. Ludwig M. Heindl, Herrn Dr. med. Alexander C. Rokohl, Herrn Dr. med. Yongwei Guo, Herrn Dr. med. Wanlin Fan und von mir zusammen ausgewertet.

Erklärung zur guten wissenschaftlichen Praxis:

Ich erkläre hiermit, dass ich die Ordnung zur Sicherung guter wissenschaftlicher Praxis und zum Umgang mit wissenschaftlichem Fehlverhalten (Amtliche Mitteilung der Universität zu Köln AM 132/2020) der Universität zu Köln gelesen habe und verpflichte mich hiermit, die dort genannten Vorgaben bei allen wissenschaftlichen Tätigkeiten zu beachten und umzusetzen.

Köln, den

Xincen Hou

Unterschrift: .....

ACKNOWLEDGEMENTS

The blooming and withering of flowers follow nature's way; meetings and partings are destined to have their time. As I come to the end of this journey, I find myself deeply grateful to many individuals who have supported and guided me throughout this experience.

First and foremost, I would like to express my deepest gratitude to my supervisor, Professor Ludwig M. Heindl. Your guidance, expertise, and unwavering support have been instrumental in completing this dissertation. Your commitment to academic excellence, insightful feedback, and patient mentorship have inspired me to delve deeper into my research and have significantly enhanced the quality of my work. I am profoundly grateful for the opportunity to work under your supervision and for all the invaluable lessons I have learned from you.

I would also like to thank Dr. Alexander C. Rokohl for his invaluable insights, critical evaluations, and constructive suggestions during my doctoral studies. His guidance and encouragement have been crucial in keeping me motivated and inspired. I would like to thank my colleagues, Guo Yongwei, Fan Wanlin, Ju Sitong, Ju Xiaojun, Li Xueting, Hang Xu, and all my colleagues for their support throughout this journey. The camaraderie and shared experiences we have had in the lab have made this journey much more enjoyable and fulfilling. Thank you for your teamwork, knowledge sharing, and the countless moments of laughter that made this challenging journey more bearable.

Gratitude is also extended to my friends, Zhang Jing and Feng Yuan, for their unwavering support and encouragement. Your friendship has been a constant source of comfort and joy, offering the emotional support necessary to persevere. Thank you

for always being there to celebrate my achievements and to support me through the challenges.

I am grateful to the China Scholarship Council for its financial support, which provided a stable foundation for my life and research. This support enabled me to complete my doctoral studies and broadened my horizons.

I am also deeply indebted to my family, especially my parents, for their unconditional support, understanding, and love throughout this challenging journey. Your constant encouragement has been a source of strength, and your belief in me has been my greatest motivation. I also wish to thank my fiancé, Xipeng Tao, for enduring support during this time. Though separated by thousands of miles, we shared joy and weathered hardships together. Your love and caring have been my refuge during this challenging period. Finally, I extend my gratitude to myself for the dedication and perseverance I brought to the research. The past three years spent in a foreign country have been a period of personal growth and development. I am grateful for the strength and fortitude I have gained through this experience.

While it is not feasible to mention everyone who has contributed to my doctoral dissertation, I sincerely thank all those who have impacted and supported my academic journey and personal development. Their encouragement and assistance have been instrumental in making this achievement possible, and I am profoundly grateful for their support.

Dedication

To my family and friends

TABLE OF CONTENTS

ABBREVIATIONS

Abbreviation	Full Form
3D	Three-dimensional
BCC	basal cell carcinoma
SCC	squamous cell carcinoma
SGC	sebaceous gland carcinoma
2D	Two-dimensional
MCC	Merkel cell carcinoma
ICC	intraclass correlation coefficient
MAD	mean absolute deviation
TEM	technical error of measurement
rTEM	relative TEM
REM	relative error of measurement
3D	Three-dimensional
BCC	basal cell carcinoma

1. SUMMARY

In this study, we utilized three-dimensional (3D) stereophotogrammetry to quantify the surface area of diverse tumors in the periocular region, assessing the reproducibility of these measurements. We collected 3D facial images from 150 patients diagnosed with periocular tumors. All tumors underwent classification according to their diameter, shape, color, location, surface texture, distance from the eyelid margin, clarity of boundaries, and histological characteristics. Following this, the surface area and volume of the tumor models were quantified, and intra-rater and inter-rater reproducibility was assessed.

The results showed overall high reliability in area measurements, with intra-rater and inter-rater intraclass correlation coefficients (ICCs) of 0.998 and 0.974, respectively. The mean absolute difference (MAD) was 0.63 and 0.40 mm^2, and the relative measurement error (REM) was 1.94% and 1.22%, respectively. The technical error of measurement (TEM) was 2.29 and 7.81 mm^2, and the relative technical error of measurement (rTEM) was 6.95% and 23.76%, respectively. Four factors influencing reliability were identified: tumor diameter, color, location, and boundary clarity. Tumors with a diameter greater than 5 mm, brownish-black in color, located at the lateral canthus, upper eyelid, and lower eyelid, with clear margins, exhibited better reliability. For tumor volume measurement, the intra-rater and inter-rater ICC estimates were 0.974 and 0.907, indicating excellent reliability. The MAD for intra-rater and inter-rater measurements was below 2 mm^3, specifically 1.44 mm^3 and 1.41 mm^3. The intra-rater TEM was 13.90 mm^3, and the inter-rater TEM was 27.65 mm^3. REM values were favorable, with 5.16% for intra-rater and 4.80% for inter-rater measurements. However, the rTEM values were relatively poor, at 49.53% for intra-rater and 93.76% for inter-rater measurements. Three factors influencing the

reliability of tumor volume measurements were identified: tumor diameter, color, and location. For volume measurements, tumors with a diameter greater than 5 mm, located at the lateral canthus and upper eyelid, and brownish-black or red in color, showed higher reliability. In general, the reliability of tumor area measurements was superior to that of tumor volume measurements.

This study is the first to conduct a comprehensive analysis with precise measurements of periocular tumor area and volume, providing reliable data on the accuracy of measurements for tumors in this region. These results are highly valuable for the clinical evaluation of periocular tumors. Surgical intervention remains the primary treatment for periocular tumors. The tumor area and volume play a critical role in determining the extent of preoperative skin excision, guiding the selection of the most suitable surgical approach, and assessing the prognosis, which is essential for the functional and aesthetic recovery of the eyelids post-surgery. Traditionally, clinical evaluations have mainly relied on measuring tumor diameter, which offers a limited assessment. Incorporating tumor area measurement into preoperative evaluations could greatly improve accuracy. Due to the complex periocular anatomy, small changes in tumor size can be difficult to detect visually. In these cases, stereophotogrammetry can be utilized for patient follow-up, facilitating the detection of subtle size changes and improving the planning of subsequent treatment strategies.

2. ZUSAMMENFASSUNG

In dieser Studie haben wir dreidimensionale (3D) Stereofotogrammetrie verwendet, um die Oberflächenfläche verschiedener Tumore im periokularen Bereich zu quantifizieren und die Reproduzierbarkeit dieser Messungen zu bewerten. Wir sammelten 3D-Gesichtsaufnahmen von 150 Patienten mit diagnostizierten periokularen Tumoren. Die Tumore wurden nach ihrem Durchmesser, ihrer Form, Farbe, Lage, Oberflächenstruktur, Entfernung vom Lidrand, Randklarheit und histologischen Merkmalen klassifiziert. Anschließend wurden die Oberflächenfläche und das Volumen der Tumormodelle quantifiziert, und die intra- und interrater Reproduzierbarkeit wurde bewertet.

Die Ergebnisse zeigten eine insgesamt hohe Zuverlässigkeit bei der Flächenmessung, mit Intraklassen-Korrelationskoeffizienten (ICC) von 0,998 (intra-rater) und 0,974 (inter-rater). Die durchschnittliche absolute Differenz (MAD) betrug 0,63 und 0,40 mm^2, und der relative Messfehler (REM) lag bei 1,94% bzw. 1,22%. Der technische Messfehler (TEM) betrug 2,29 und 7,81 mm^2, und der relative technische Messfehler (rTEM) betrug 6,95% bzw. 23,76%. Vier Faktoren, die die Zuverlässigkeit beeinflussten, wurden identifiziert: Tumordurchmesser, Farbe, Lage und Klarheit der Grenzen. Tumore mit einem Durchmesser von mehr als 5 mm, braun-schwarzer Farbe, die sich am lateralen Augenwinkel, am Oberlid oder Unterlid befinden und klare Ränder aufweisen, zeigten eine bessere Zuverlässigkeit. Bei der Volumenmessung von Tumoren wurden intra- und interrater ICC-Schätzungen von 0,974 und 0,907 ermittelt, was auf eine hervorragende Zuverlässigkeit hinweist. Der MAD bei intra- und interrater Messungen lag unter 2 mm^3, konkret bei 1,44 mm^3 und 1,41 mm^3. Der intra-rater TEM betrug 13,90 mm^3 und der inter-rater TEM 27,65 mm^3. Die REM-Werte waren günstig, mit 5,16% bei intra-rater und 4,80% bei inter-rater

Messungen. Die rTEM-Werte hingegen waren relativ schlecht, mit 49,53% für intra-rater und 93,76% für inter-rater Messungen. Drei Faktoren, die die Zuverlässigkeit der Tumorvolumenmessung beeinflussten, wurden identifiziert: Tumordurchmesser, Farbe und Lage. Für Volumenmessungen zeigten Tumore mit einem Durchmesser von mehr als 5 mm, die sich am lateralen Augenwinkel und Oberlid befinden und braun-schwarz oder rot sind, eine höhere Zuverlässigkeit. Insgesamt war die Zuverlässigkeit der Flächenmessung von Tumoren der der Volumenmessung überlegen.

Diese Studie stellt die erste umfassende Analyse mit präzisen Messungen von periokularer Tumorfläche und -volumen dar und liefert zuverlässige Daten zur Messgenauigkeit von Tumoren in diesem Bereich. Diese Ergebnisse sind von großem Wert für die klinische Bewertung periokularer Tumoren. Der chirurgische Eingriff bleibt die primäre Behandlungsmethode für periokulare Tumoren. Die Tumorfläche und das Volumen spielen eine entscheidende Rolle bei der Bestimmung des Umfangs der präoperativen Hautexzision, der Auswahl des geeignetsten chirurgischen Ansatzes und der Beurteilung der Prognose, was für die funktionelle und ästhetische Wiederherstellung der Augenlider nach der Operation von entscheidender Bedeutung ist. Traditionell basieren klinische Bewertungen hauptsächlich auf der Messung des Tumordurchmessers, was eine begrenzte Beurteilung darstellt. Die Einbeziehung der Tumorflächenmessung in präoperative Bewertungen könnte die Genauigkeit erheblich verbessern. Aufgrund der komplexen periokularen Anatomie sind kleine Veränderungen der Tumorgröße visuell schwer zu erkennen. In solchen Fällen kann die Stereofotogrammetrie zur Nachsorge von Patienten verwendet werden, um subtile Größenänderungen leichter zu erkennen und die Planung nachfolgender Behandlungsstrategien zu verbessern.

3. INTRODUCTION

3.1 Periocular Tumors

3.1.1 Benign Tumors

The periocular region is critically important and simultaneously fragile within the facial anatomy. Despite its relatively small surface area, it ranks among the skin areas most frequently exposed to sunlight. Besides the subcutaneous fat layer, this region encompasses all other skin structures, which can be origins for various benign tumors. Benign tumors in the periocular area are common and diverse, including chalazion, epidermoid inclusion cysts, seborrheic keratosis, and apocrine cystadenoma, often causing cosmetic concerns or ocular irritation[1,2]. Benign tumors are more prevalent than malignant ones and tend to present at a younger age, with a higher incidence observed in the upper eyelid[3-5].

3.1.2 Malignant Tumors

The skin in the periocular region is thin and particularly sensitive to ultraviolet (UV) radiation and various irritants. Consequently, this area has a notably high incidence of skin cancers, with an estimated rate of around 15 cases per 100,000 individuals annually [6,7]. Approximately 5% to 10% of all skin cancers develop on the eyelids, most commonly as basal cell carcinoma (BCC), followed by squamous cell carcinoma (SCC), sebaceous gland carcinoma (SGC), Merkel cell carcinoma, and melanoma[8,9]. Malignant tumors in the periocular region not only pose aesthetic challenges but also potentially impair ocular function, significantly impacting patients' vision and quality of life. Due to the anatomical and functional significance, aesthetic considerations are paramount in treatment planning. Preserving as much periocular tissue as possible while ensuring safe margins during surgical interventions presents a challenge for ophthalmologists and plastic surgeons. Accurate preoperative measurement of tumor

dimensions plays a crucial role in tailoring surgical strategies, facilitating optimal outcomes and patient satisfaction.

In the periocular region, basal cell carcinoma (BCC) represents the most prevalent type of malignant tumor, comprising 90% to 95% of cases in Western countries[1]. BCC originates from the basal layer of the epidermis and typically appears as a pearly, raised lesion with telangiectasia, elevated margins, and central ulceration[9]. A definitive diagnosis of malignancies requires histopathological evaluation, as clinical presentations can vary widely, making a pathologic study essential. Biopsies should be performed on all suspicious lesions. Histopathologic subtypes of BCC include superficial, infiltrative, nodular, and tumors with adnexal differentiation[10]. Several risk factors contribute to BCC development, including exposure to sunlight, immunosuppression, thermal injury scars, fair skin, arsenic exposure, smoking (particularly in women), older age, and ionizing radiation[6,7,11]. BCC predominantly affects the lower eyelid, representing 50% to 60% of cases, followed by the medial canthus at 25% to 30%, with the upper lid and lateral canthus being less commonly involved, accounting for 15% and 5% of cases, respectively[1,12,13]. The upper eyelid's lower frequency of involvement is likely due to the protective effect of the brow[14].BCC primarily spreads through direct invasion of adjacent tissues and, in rare cases, can extend into the orbit. Metastasis is uncommon in BCC. Intracranial BCC mortality, estimated at 3%, is typically associated with neglected or inadequately treated tumors that have extended intracranially[6].

Following BCC, squamous cell carcinoma (SCC) ranks as the second most prevalent skin malignancy, accounting for 20% to 25% of nonmelanoma skin cancers and 5% to 10% of eyelid malignancies[15,16].SCC may present as a painless nodule or plaque with

irregular margins, induration, keratinization, and ulceration. Precancerous lesions for SCC include actinic keratosis, Bowen's disease, and keratoacanthoma[16].SCC predominantly affects older adults, especially those over the age of 60, and occurs more frequently in men than women[17]. The main risk factors include fair skin and prolonged sun exposure, making SCC uncommon in Black, Asian, and Hispanic populations but more prevalent among Caucasians. UVB radiation is the most significant carcinogenic factor, resulting in higher incidence rates among individuals with outdoor exposure[18]. Other risk factors include actinic damage, previous SCC, and chronic skin injuries such as ulcers, burns, sinus tracts, vaccination scars, and chronic skin diseases[16,18].SCC is characterized by its tendency for perineural and vascular invasion, deep subclinical spread, and rapid growth potential[19]. Unlike BCC, SCC has a higher probability of orbital invasion and commonly spreads through lymphatic and hematologic routes to regional lymph nodes and distant sites. When SCC metastasizes locally or distantly, the prognosis worsens significantly, often necessitating additional treatments such as radiation or chemotherapy along with surgical excision[20,21].

Melanomas of the periocular are exceedingly rare, accounting for approximately 1% of all eyelid malignancies and less than 1% of cutaneous malignant melanomas[20,22]. Eyelid melanoma can present as an isolated lesion or result from the spread of conjunctival melanoma across the mucocutaneous junction or from other distant cutaneous sites[22]. The American Cancer Society established the ABCDE criteria to aid in early melanoma diagnosis: "A" stands for asymmetry of the lesion, "B" for irregular borders, "C" for color variations, "D" for diameter (usually greater than 6 mm), and "E" for evolution in appearance. Lesions exhibiting these characteristics warrant further evaluation for malignancy. Biopsy remains the gold standard for assessing

invasion depth, which correlates directly with prognosis in all forms of malignant melanoma. Melanoma classification traditionally relies on clinicopathologic features based on the morphologic growth stage. According to the World Health Organization, the four primary subtypes are superficial spreading melanoma (30% to 60%), lentigo malign melanoma (10% to 40%), nodular melanoma (15% to 35%), and acral lentiginous melanoma (5% to 10%)[23]. Melanomas located near the eyelid margin, conjunctiva, fornix, fossa, and caruncle are associated with higher recurrence and metastasis rates[24]. Ultraviolet B radiation plays a pivotal role in the development of eyelid melanoma. Additional risk factors encompass a familial history of melanoma, multiple atypical nevi, severe sun exposure during childhood, fair skin, red hair, freckles, and advanced age[22].

Sebaceous gland carcinoma (SGC), with an estimated incidence of 1 to 2 cases per million people annually, is the third most prevalent eyelid carcinoma, following basal cell carcinoma and squamous cell carcinoma[25]. However, in South Asia, it is reported to be the most common periocular tumor[26]. SGC typically occurs in older individuals, with the median age of diagnosis between 70 and 73 years[25]. Some studies suggest that men are 1.35 to 1.4 times more likely to develop SGC than women, although other research indicates a higher incidence among women[27].SGC most commonly arises from the Meibomian glands along the eyelid margin or the Zeis glands associated with individual eyelashes, but it can also originate from the caruncle or pilosebaceous structures of the hair follicles in the eyebrows[28]. Clinically, periocular SGC often presents as a painless papule, rough nodule, or cystic lesion that rapidly increases in size. Misdiagnosis is common, with up to two-thirds of cases initially mistaken for benign conditions such as chalazion, blepharitis, or lid margin conjunctivitis, leading to delayed diagnosis and potentially poor outcomes[29].The

upper eyelid is the most frequently affected site, but SGC can also involve the lower eyelid, cornea, conjunctiva, caruncle, medial and lateral canthi, and even spread more diffusely. SGC has the potential to metastasize through lymphatic or hematogenous routes or directly invade the orbit[30].Therefore, early detection of SGC is vital for improved prognosis.

Merkel cell carcinoma (MCC) is an uncommon but highly aggressive neuroendocrine tumor characterized by a significant risk of local metastasis and recurrence[9]. MCC typically presents as asymptomatic solitary nodules that are pale red or purplish, often with telangiectatic vessels and ulceration. These lesions frequently occur in the upper eyelid, commonly near the lid margin, and can lead to partial or complete eyelash loss. Risk factors for MCC include advanced age, immunosuppression, ultraviolet exposure, and infection with polyomavirus, which is linked to approximately 80% of cases[31]. Due to its rarity, MCC can be mistaken for chalazion, keratoacanthoma, or basal cell carcinoma, as it often exhibits rapid growth with noticeable changes within weeks or months. Consequently, the biopsy is crucial to avoid clinical misdiagnosis. MCC has a high likelihood of spreading to regional lymph nodes, with two-thirds of patients reporting lymph node metastases within 18 months of diagnosis and one-third experiencing distant metastases[32].Patients with positive lymph node biopsies have a recurrence rate three times higher than those without.The first two years post-diagnosis carry the greatest risk for metastasis and recurrence, although recurrence can occur at any time, necessitating lifelong monitoring[33,34].

3.2 Two-dimensional(2D) Anthropometry

Traditional research on measuring periocular tumor size primarily relied on traditional direct anthropometry or 2D imaging tools such as standardized photographs.

Two-dimensional imaging methods have been employed in anthropometric studies for over four decades[35]. These images capture static representations of dynamic subjects, requiring participant cooperation during the capture process. Due to their non-invasive nature, speed, and low cost, 2D imaging techniques are often preferred over direct physical measurements[36]. Despite their widespread use in facial measurements[37], 2D imaging faces challenges such as magnification errors, distortions, and variability introduced by factors like varying object-to-camera distances and inconsistent lighting conditions[38]. Moreover, this approach only allows for planar contour analysis, limiting its ability to provide a comprehensive assessment of the full three-dimensional structure of the face, particularly when evaluating curvature、surface area and volume.

3.3 Three-dimensional (3D) Stereophotogrammetry

In 1987, the Loughborough Anthropometric Shadow Scanner (LASS) was designed and developed for automated anthropometry[39]. Over the following decades, advancements in stereophotogrammetry enabled the clinical application of 3D imaging. 3D imaging technology captures high-resolution surface shapes, contours, and colors non-invasively by taking simultaneous photos from different angles with high-resolution, fast-capturing cameras and combining them into a 3D image. The accompanying software not only allows visualization and analysis but also enables measurement of linear distances, angles, areas, and volumes[40,41]. This method offers advantages such as high color resolution, absence of motion artifacts, rapid 3D surface morphology reconstruction, and archiving capability for subsequent analysis[42,43].

Stereophotogrammetry encompasses various formats, and some studies have explored the clinical applications of 3D stereophotogrammetry imaging systems, such

as the Vectra H1-270 camera (Canfield Imaging Systems, Fairfield, NJ, USA)[44], 3D Vectra® H1 (Canfield Scientific Inc., Parsippany, NJ, USA)[45] , Vectra H2 (Canfield Imaging, Parsippany, NJ, USA)[46,47], and the 3dMD Head System (3dMD LLC, Atlanta, GA, USA) [48]. Additionally, research has indicated the potential use of smartphone applications for facial scanning [49,50].

The VECTRA M3 3D imaging system (Canfield Scientific, Inc., Parsippany, NJ, USA) used in this study features a capture system with a 1.2 mm geometric resolution. In recent years, three-dimensional systems have gradually replaced 2D systems and traditional anthropometry and have been widely used in morphological assessments of the facial region, making them one of the most promising tools for evaluating facial soft tissues. Several studies have demonstrated the high precision and accuracy of 3D stereophotogrammetry[51-54]. Unfortunately, there is currently a lack of studies specifically addressing the measurement of periocular tumor areas. Consequently, the reliability of periocular tumor area measurements remains insufficiently validated.

For now, there is limited data available on the use of 3D stereophotogrammetry for the precise measurement of periocular tumors, particularly regarding the reproducibility of such measurements. Accurate and reproducible measurement techniques are essential for clinical decision-making, especially in the periocular region, where tumors can impact both function and aesthetics. Traditional measurement methods, such as manual calipers, often lack the precision and consistency needed to make informed surgical or treatment decisions. Our study addresses this gap by providing quantitative evidence of the high reproducibility of 3D stereophotogrammetry in assessing

periocular tumors, which, to our knowledge, has not been comprehensively studied in the current literature.

Reproducibility is crucial because it ensures that measurements of tumor size and characteristics are reliable over time and across different clinicians. Inconsistent measurements could lead to variations in treatment planning, such as the extent of surgical excision or the need for additional interventions. For example, in periocular tumors, even small discrepancies in measurement can affect decisions regarding surgical margins, reconstructive strategies, and postoperative monitoring. By validating the reproducibility of the measurement technique, we aim to contribute to more standardized and reliable treatment protocols, ultimately improving patient outcomes.

3.4 Aims

The objective of this study is to assess the reproducibility of measurements for the area and volume of periocular tumors using the Vectra M3 3D imaging system, providing evidence for the reliability of stereophotogrammetry in quantifying periocular tumor size. The findings of this research hold significant implications for preoperative diagnosis, surgical planning, and postoperative assessment of outcomes in patients.

4. MATERIAL AND METHODS

4.1 Participants

This study enrolled 150 patients with periocular tumors. They underwent stereophotogrammetry using the VECTRA M3 3D imaging system (Canfield Scientific, Inc., Fairfield, NJ, USA) at the Department of Ophthalmology, University of Cologne, from January 2022 to January 2024. Photographs of the patients were taken using the VECTRA M3 3D imaging system. Prior to imaging, patients were instructed to fully expose their faces. To ensure image clarity, no makeup was permitted on the face. Patients were seated in front of the camera with their heads held upright and facial expressions relaxed. All photographs were taken under consistent lighting conditions by an experienced researcher and photographer who had received standardized training. Inclusion criteria were as follows: patients were stationary during photography, had a natural expression, fully exposed faces, upright heads, and were seated in front of the camera; the tumor was located around the eye; the 3D image was clear; and the face was free of makeup and decorations. Patients with facial deformities, anomalies, trauma, or skin diseases were excluded. Observational data included age, gender, lesion location, and tumor characteristics. Informed consent was obtained in writing from each participant. This research adheres to the principles outlined in the Declaration of Helsinki and received approval from the University of Cologne Ethics Committee (Number: 17-199).

4.2 Measurements and Data Analysis

Two independent raters measured each image. After enlarging each image to an appropriate scale, markers were carefully placed at the edges of the lesion. The lesion's area was delineated by connecting the centers of these markers, ensuring the outline completely encompassed the entire lesion. Area measurements were

computed using Vectra software (Canfield Scientific, Inc., Fairfield, NJ, USA). Rater 1 performed duplicate measurements for each image, while rater 2 conducted a single measurement per image, referred to as Measurements 1.1, 1.2, and 2.1, respectively (Figure 1).

Figure 1 VECTRA M3 dimension and Patients with Periocular Tumors Captured Using the VECTRA M3 Imaging System

Reliability analyses for intra-rater and inter-rater assessments were performed by comparing measurements 1.1 with 1.2 and measurements 1.1 with 2.1. Five indicators were employed to evaluate the reliability of stereophotography: intraclass correlation coefficient (ICC), mean absolute deviation (MAD), technical error of measurement (TEM), relative error of measurement (REM), and relative TEM (rTEM). Higher ICC values generally indicate smaller differences, while lower TEM, REM, rTEM, and MAD values suggest greater reliability. ICC is typically used to evaluate consistency between measurements, with ICC > 0.9 considered excellent, 0.75 to 0.9 as good, 0.5 to 0.75 as moderate, and ICC < 0.5 as poor[55].

In prior studies, the acceptable error threshold for both MAD and TEM within the maxillofacial regions was established at less than two units[56]. Despite this, because of the smaller size of the periocular region, some studies have recommended that the acceptable error threshold for MAD and TEM can be set to below one unit [57,58]. For REM and rTEM, thresholds of ≥10%, 7% to 9.9%, 4% to 6.9%, 1% to 3.9%, and <1% are considered poor, moderate, good, very good, and excellent, respectively[55,57,59].

Analysis was conducted using SPSS 26.0 (IBM Corp., Armonk, NY, USA). Continuous variables following normal distribution were presented as mean ± standard deviation (SD), whereas variables with non-normal distributions were described using median (interquartile range). The chi-squared test was used to analyze categorical data. The Kolmogorov-Smirnov test was employed to determine if the data followed a normal distribution. The t-test was used for continuous variables if the data were normally distributed. In contrast, the non-parametric Mann-Whitney U test was used if the data were not normally distributed. A p-value < 0.05 was considered statistically significant. Factors influencing measurement reliability were analyzed using R version 4.2.2(R Foundation for Statistical Computing). Significant variables were identified through lasso regression with 10-fold cross-validation. Following this analysis, bar charts and radar charts depicting the results were created using GraphPad Prism 8 (GraphPad Software Inc., San Diego, California, USA) and Excel.

5. RESULTS

5.1 Tumor characteristics

Our study included 150 patients with periorbital tumors, collecting a total of 175 tumors. Among them, 46.9% (82 tumors) were from males and 53.1% (93 tumors) were from females. The median age of the patients was 64 years. Paired t-tests or Wilcoxon signed-rank tests showed no statistically significant differences between intra-rater and inter-rater measurements. Table 1 presents the detailed characteristics of the tumors.

Table 1 The demographic and clinical features of patients with eyelid tumors

	Total n = 175	p-value			
		Intra-rater(Area 1.1 v 1.2)	Inter-rater(Area 1.1 v 2.1)	Intra-rater(Volume 1.1 v 1.2)	Inter-rater(Volume 1.1 v 2.1)
Gender					
Male	82 (46.9%)	0.823	0.932	0.971	0.867
Female	93 (53.1%)	0.905	0.827	0.815	0.812
Age (years)	64	0.803	0.876	0.909	0.993
Median (IQR)	(54-79)				
Laterality					
Right	98 (56.0%)	0.897	0.743	0.981	0.817
Left	77 (44.0%)	0.782	0.885	0.813	0.803
Location					
Upper eyelid	49 (28.0%)	0.941	0.89	0.98	0.637
Lower eyelid	93 (53.1%)	0.754	0.986	0.885	0.623
Medial canthal region	25 (14.3%)	0.946	0.503	0.854	0.915
Lateral canthal region	8 (4.6%)	1	0.916	0.793	0.916
Tumor histologic types					
Benign	117 (66.9%)	0.804	0.754	0.918	0.732
Malignant	58 (33.1%)	0.895	0.847	0.978	0.627
Size (mm)	5.08	0.803	0.876	0.909	0.993
Median (IQR)	(3.21-8.38)				
Shape					
Round or roundish	135 (77.1%)	0.828	0.864	0.935	0.88
Others	40 (22.9%)	0.874	0.969	0.92	0.765

Distance to eyelashes					
0mm	117 (66.9%)	0.766	0.772	0.885	0.989
＞0mm	58 (33.1%)	0.947	0.551	0.982	0.956
Color					
Red	45 (25.7%)	0.904	0.888	0.932	0.672
Flesh-colored	93 (53.1%)	0.95	0.782	0.926	0.805
Yellow	20 (11.4%)	0.626	0.433	0.808	0.935
Brownish-black	17 (9.8%)	0.877	1	0.877	0.959
Border					
Well-defined	137 (78.3%)	0.807	0.852	0.913	0.846
Ill-defined	38 (21.7%)	0.893	0.934	0.983	0.901
Surface Texture					
Skin texture	41 (23.4%)	0.806	0.707	0.959	0.386
Smooth	83 (47.4%)	0.882	0.606	0.812	0.625
Rough	51 (29.2%)	0.928	0.928	0.987	0.976

5.2 Area of Periocular Tumors

5.2.1 Comprehensive Reliability Assessment

The intra-rater and inter-rater ICC estimates are excellent, at 0.998 and 0.974, respectively. The TEM for intra-rater and inter-rater measurements were 2.29 mm^2 and 7.81 mm^2. The intra-rater and inter-rater MAD were less than 2 mm^2, measuring 0.63 mm^2 and 0.40 mm^2, respectively. The intra-rater and inter-rater REM are very good, at 1.94% and 1.22% respectively. The intra-rater rTEM is good (6.95%), whereas the inter-rater rTEM is poor (23.76%). Overall, except for TEM and inter-rater rTEM, all indicators demonstrate good reliability of the measurement results.

5.2.2 Factors Influencing Reliability

Due to the varying characteristics of different tumors, the reliability of measurement results may differ across tumors. To identify the factors that most significantly impact measurement reliability, we employed LASSO regression combined with 10-fold cross-validation to screen nine factors: age, diameter, shape, color, location, surface texture, distance from the eyelid margin, clarity of boundaries, and histological

characteristics (Figure 2). Subsequently, a random forest analysis was employed to prioritize these factors, revealing that diameter, color, location, and boundary were the most significant (Figure 3). Lastly, a detailed reliability analysis focused on these key factors.

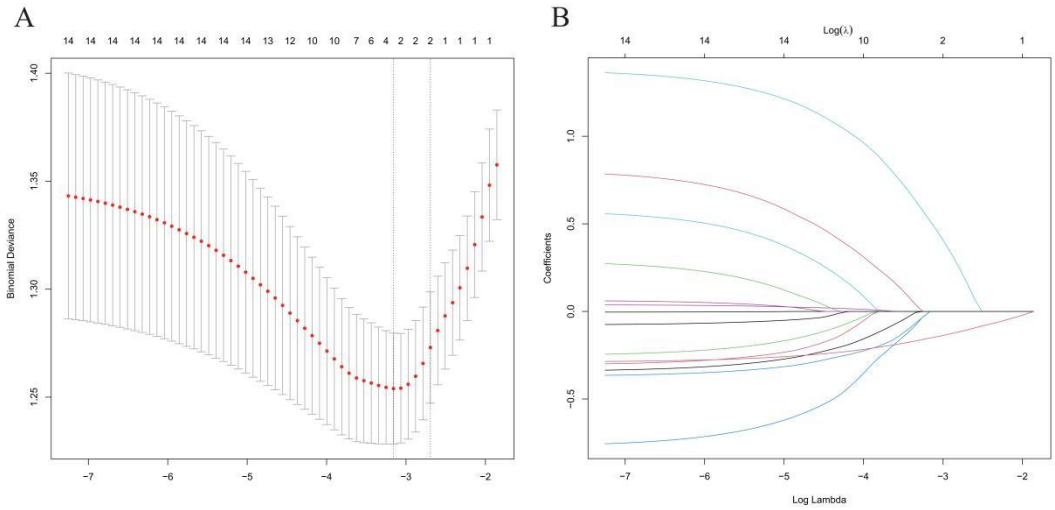

Figure 2. LASSO logistic regression was used for variable selection: (A) Ten-fold cross-validation for tuning parameter selection in the LASSO model. The plot shows the binomial deviance versus log (λ), where λ is the tuning parameter. (B) The LASSO coefficient profiles are displayed, with the optimal tuning parameter (λ) determined through 10-fold cross-validation based on the minimum criteria.

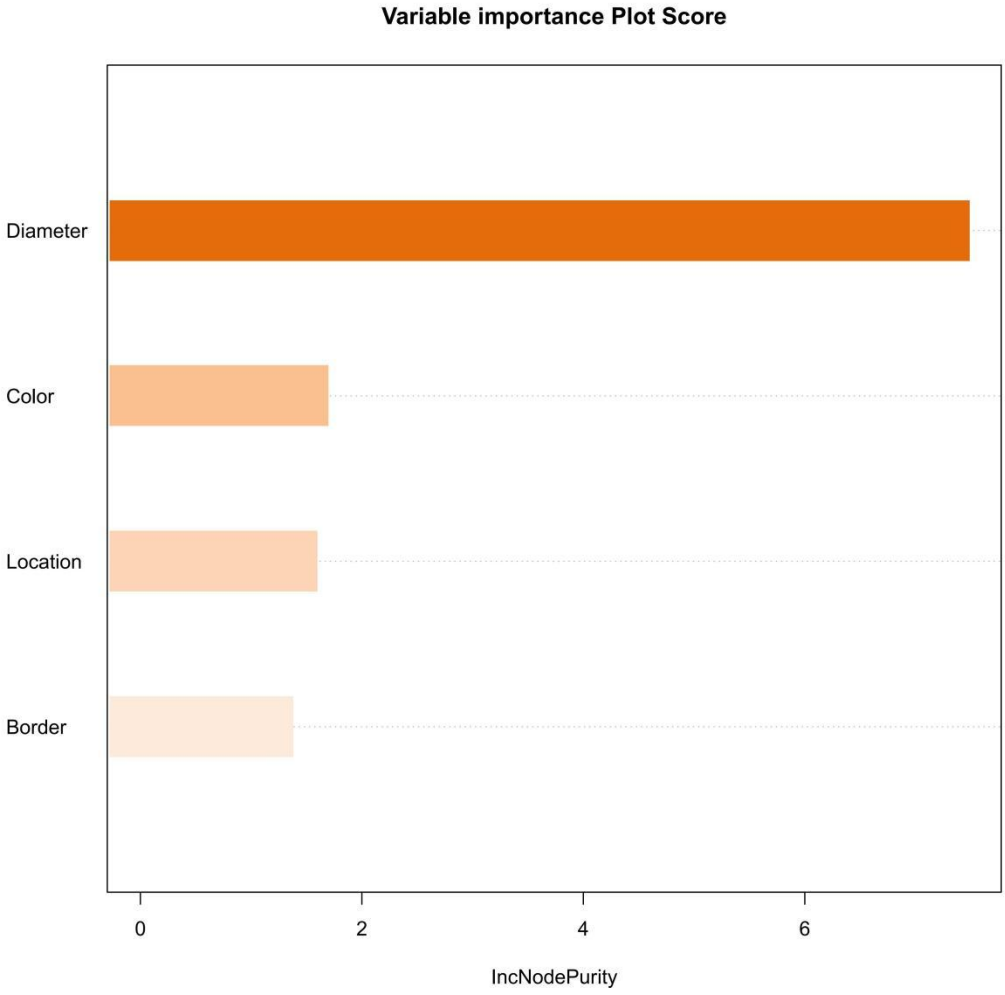

Figure 3. Feature importance ranks in random forest. The factors affecting the reliability of tumor area measurements, ranked in order of importance from highest to lowest, are diameter, color, tumor location, and boundary.

5.2.3 Diameter

Since tumor diameter is a continuous variable, the ROC analysis was employed to establish an optimal cutoff value of 5 mm for effective classification and comparison. As a result, diameters were divided into ≤5 mm and >5 mm. For tumors with a diameter greater than 5 mm, both intra-rater and inter-rater ICC were excellent (0.998 and 0.977). REM was very good, and the intra-rater and inter-rater MAD were below 2 mm^2, whereas the TEM exceeded 2 mm^2. The intra-rater and inter-rater rTEM were 4.25% (good) and 15.98% (poor). Regarding tumors with a diameter of 5 mm or less, the intra-rater MAD was less than 2 mm^2, while the TEM and inter-rater MAD were greater than 2 mm^2. The intra-rater and inter-rater ICCs were found to be good and poor (0.831 and 0.345). The intra-rater REM was 4.08% (good), while the inter-rater REM was 18.76% (poor). Both intra- and inter-rater rTEM were poor. In general, intra-rater reliability was better than inter-rater reliability. Compared to tumors with a diameter of 5 mm or less, the overall measurement reliability for tumors larger than 5 mm was higher and significantly better (Figure 4 and Figure 5).

5.2.4 Color Characteristics

Except for yellow tumors, where the inter-rater ICC was good, the intra- and inter-rater ICC for tumors of all other colors were excellent. Regarding red tumors, the inter-rater REM and rTEM were 1.57% (very good) and 22.84% (poor), whereas the intra-rater REM and rTEM were 0.83% (excellent) and 5.27% (good). The inter-rater TEM exceeded 2 mm^2, while the intra-rater TEM was less than 2 mm^2; the MAD for intra- and inter-rater measurements was 0.31 mm^2 and 0.58 mm^2. For flesh-colored tumors, the inter-rater REM was 0.26%(excellent), and the intra-rater REM was 1.75% (very good); the intra-rater rTEM was 6.60% (good), while the inter-rater rTEM was 14.81% (poor). The intra- and inter-rater MAD were 0.46 and 0.06 mm^2, respectively. The

TEM was less than 2 mm² for intra-rater measurements, at 1.75 mm², and greater than 2 mm² for inter-rater measurements, at 3.90 mm². Except for the intra-rater REM, which was good (6.59%), all measurements for yellow tumors, including intra-rater rTEM, inter-rater REM, and rTEM, were poor. The MAD and TEM exceeded 2 mm² for both intra- and inter-rater measurements. As for brownish-black tumors, the intra-rater REM (1.32%), rTEM (2.70%), and inter-rater REM (3.74%) were very good, while the inter-rater rTEM was poor. The intra-rater MAD and TEM were 0.72 mm² and 1.49 mm², respectively, while the inter-rater MAD was 2.01 mm², with a TEM of 13.17 mm². Overall, tumors with flesh-colored and brownish-black appearances exhibit higher reliability, whereas those with yellow appearances show the lowest reliability (Figure 4 and Figure 5).

5.2.5 Localization

Despite the different locations, all tumors exhibited excellent ICC. In the upper eyelid, the intra-rater REM was 0.39% (excellent), while both the inter-rater and intra-rater REM (4.05%) and rTEM (4.09%) were good, although the inter-rater rTEM was poor (18.79%). The intra-rater MAD and TEM were under 2 mm², and the inter-rater MAD and TEM were below and exceeded 2 mm², respectively. The intra-rater and inter-rater REM (3.11% and 1.90%) were very good for the lower eyelid, with the intra-rater rTEM (8.02%) being moderate and the inter-rater rTEM (23.23%) poor. The intra- and inter-rater MAD were less than 2 mm², while the TEM was greater than 2 mm². Tumors in the medial canthus had excellent intra-rater REM (0.91%) and moderate rTEM (7.38%), but poor inter-rater REM and rTEM. The intra-rater MAD was below 2 mm², and both the TEM and inter-rater MAD were greater than 2 mm². In the lateral canthus, the intra-rater REM (1.02%) and rTEM (2.26%) were very good, and inter-rater REM (0.49%) and rTEM (4.46%) were excellent and good, respectively.

The inter-rater TEM was greater than 2 mm², while the MAD and intra-rater TEM were less than 2 mm². The lateral canthus measurements generally showed the highest reliability, followed by the upper and lower eyelids, with the medial canthus having the lowest reliability (Figure 4 and Figure 5).

5.2.6 Boundary

The intra- and inter-rater ICC (0.998 and 0.972) were excellent for tumors with well-defined boundaries, with MAD under 2 mm². The intra- and inter-rater TEMs were greater than 2 mm² and less than 2 mm², respectively. The REM for intra- and inter-rater assessments were under 2%, indicating very good reliability. Additionally, the intra-rater rTEM was good, whereas the inter-rater rTEM was poor. The intra-rater and inter-rater ICC (0.996 and 0.978) were also excellent for tumors with unclear boundaries, with MAD less than 2 mm² and TEM above 2 mm². The REM for intra-rater and inter-rater were very good and excellent, respectively. Regarding rTEM, it performed poorly for inter-rater and was good for intra-rater (Figure 4 and Figure 5).

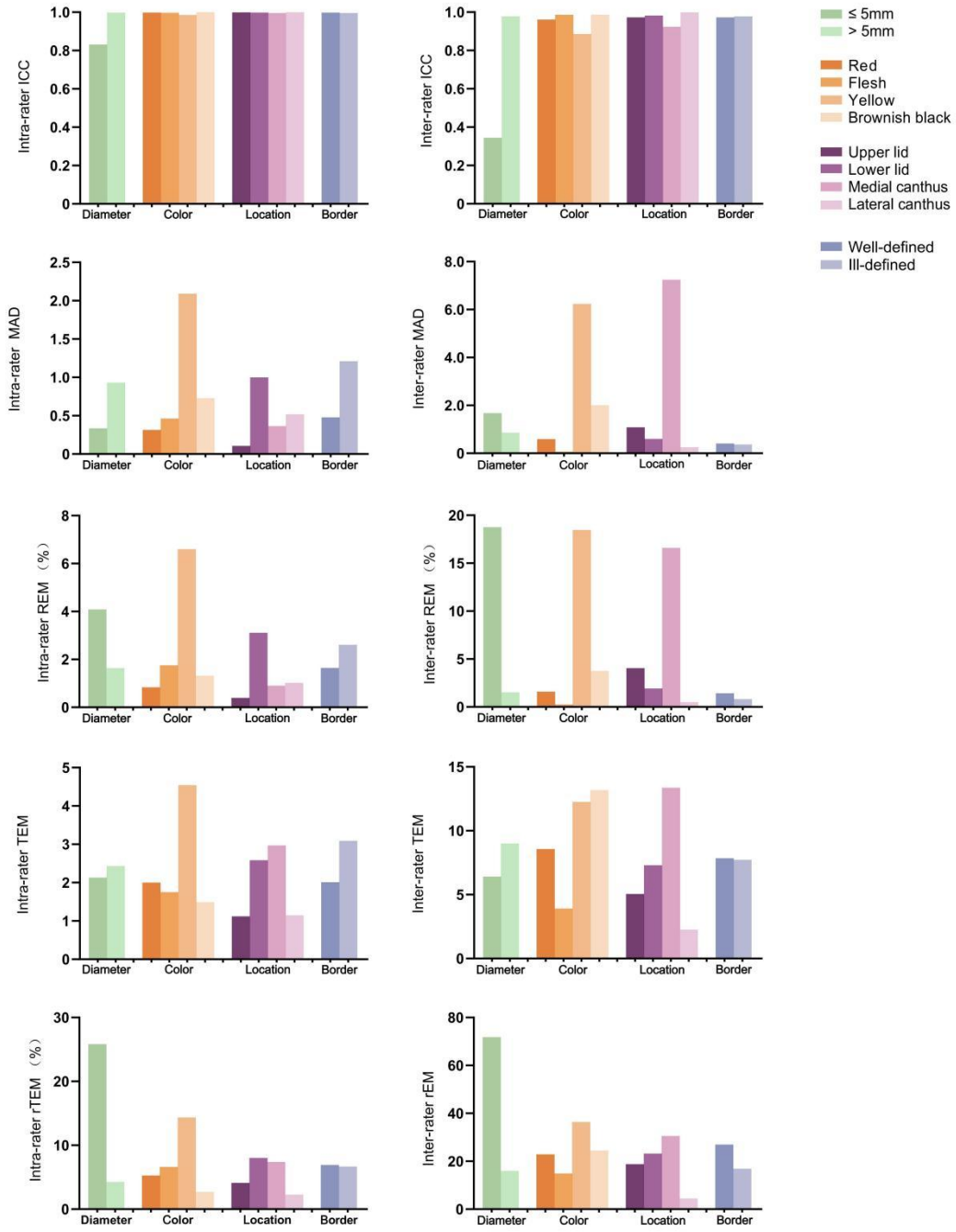

Figure 4. The bar graph shows the intra-and inter-rater reliability of tumor area measurements, including intraclass correlation coefficient (ICC), mean absolute difference (MAD), technical error of measurement (TEM), relative error of measurement (REM), and relative TEM (rTEM).

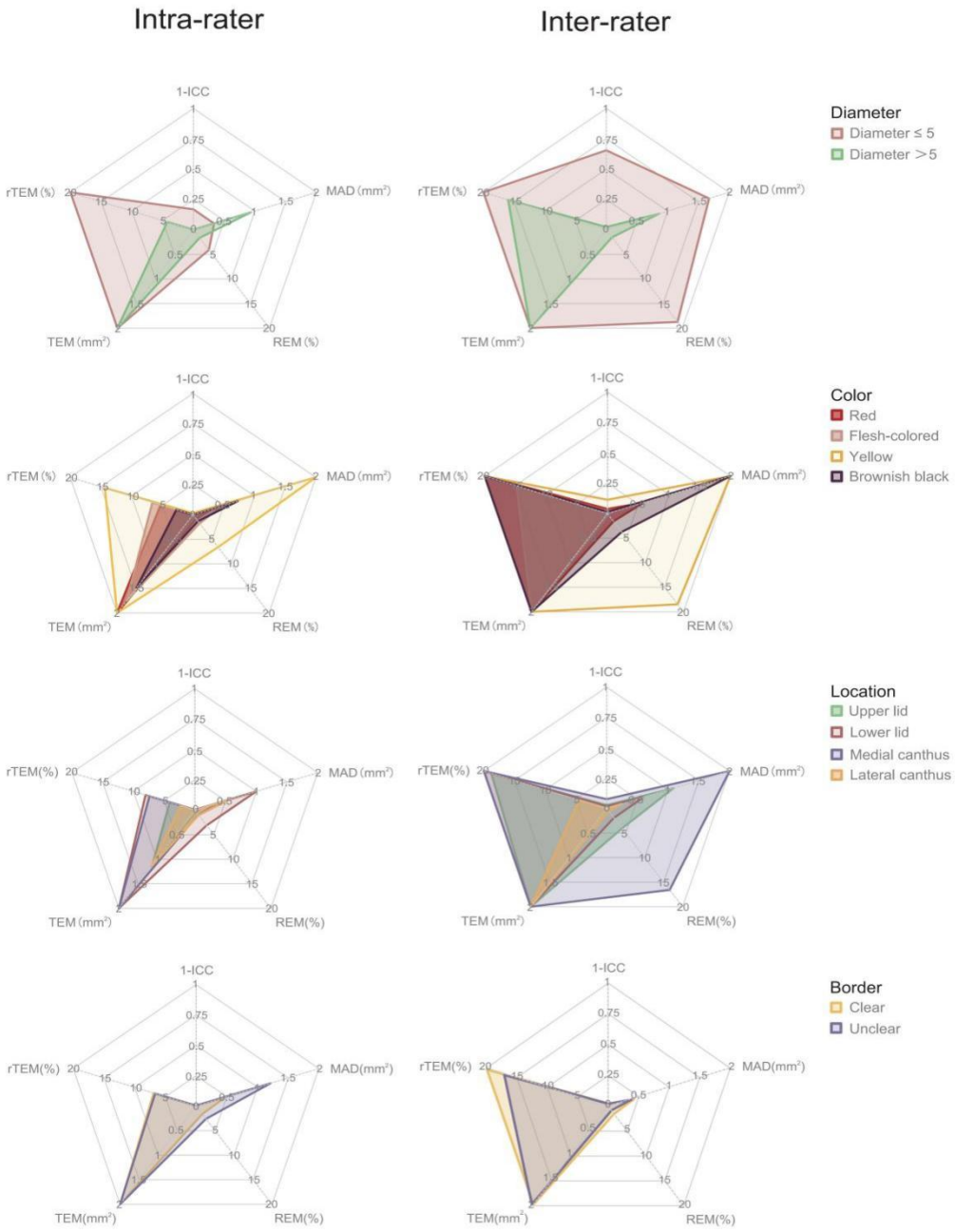

Figure 5. The radar graph offers a clearer visualization of the intra-rater and inter-rater reliability for different types of periocular tumor area measurements, displaying the intraclass correlation coefficient (1-ICC), mean absolute difference (MAD), technical error of measurement (TEM), the relative error of measurement (REM), and relative TEM (rTEM). The smaller the area enclosed by the five different parameter points, the higher the reliability.

5.3 Volume of Periocular Tumors

5.3.1 Comprehensive Reliability Assessment

The ICC estimates for intra-rater and inter-rater measurements were 0.974 and 0.907, respectively, indicating excellent reliability. The MAD for intra-rater and inter-rater measurements were both below 2 mm^3, specifically 1.44 mm^3 and 1.41 mm^3. The TEM were 13.90 mm^3 for intra-rater and 27.65 mm^3 for inter-rater measurements. The REM were good at 5.16% for intra-rater and 4.80% for inter-rater measurements. The rTEM values for intra-rater and inter-rater measurements were poor, at 49.53% and 93.76%, respectively. In general, except for TEM and rTEM, all metrics indicated good measurement reliability.

5.3.2 Factors Influencing Reliability

To identify the factors that most affect the reliability of volume measurements, we used LASSO regression combined with 10-fold cross-validation, selecting nine factors: age, diameter, shape, color, location, surface texture, distance from the eyelid margin, boundary clarity, and histological characteristics (Figure 6). Subsequently, a random forest analysis was conducted to prioritize these factors, revealing that diameter, color, and location are the most critical factors influencing the reliability of tumor volume measurements (Figure 7). Following this, we conducted a detailed reliability analysis on these key factors.

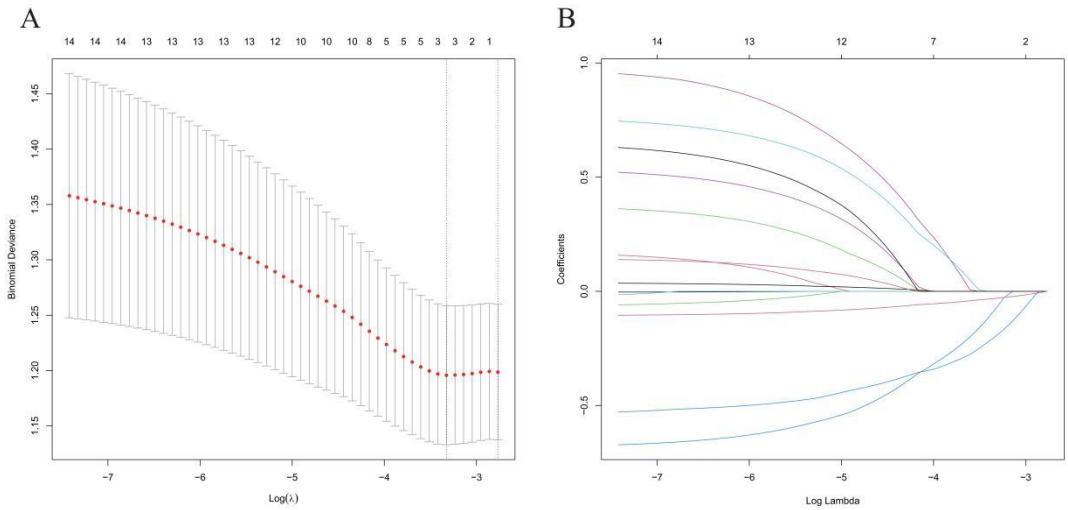

Figure 6. LASSO logistic regression was used for variable selection: (A) Ten-fold cross-validation for tuning parameter selection in the LASSO model. The plot shows the binomial deviance versus log (λ), where λ is the tuning parameter. (B) The LASSO coefficient profiles are displayed, with the optimal tuning parameter (λ) determined through 10-fold cross-validation based on the minimum criteria.

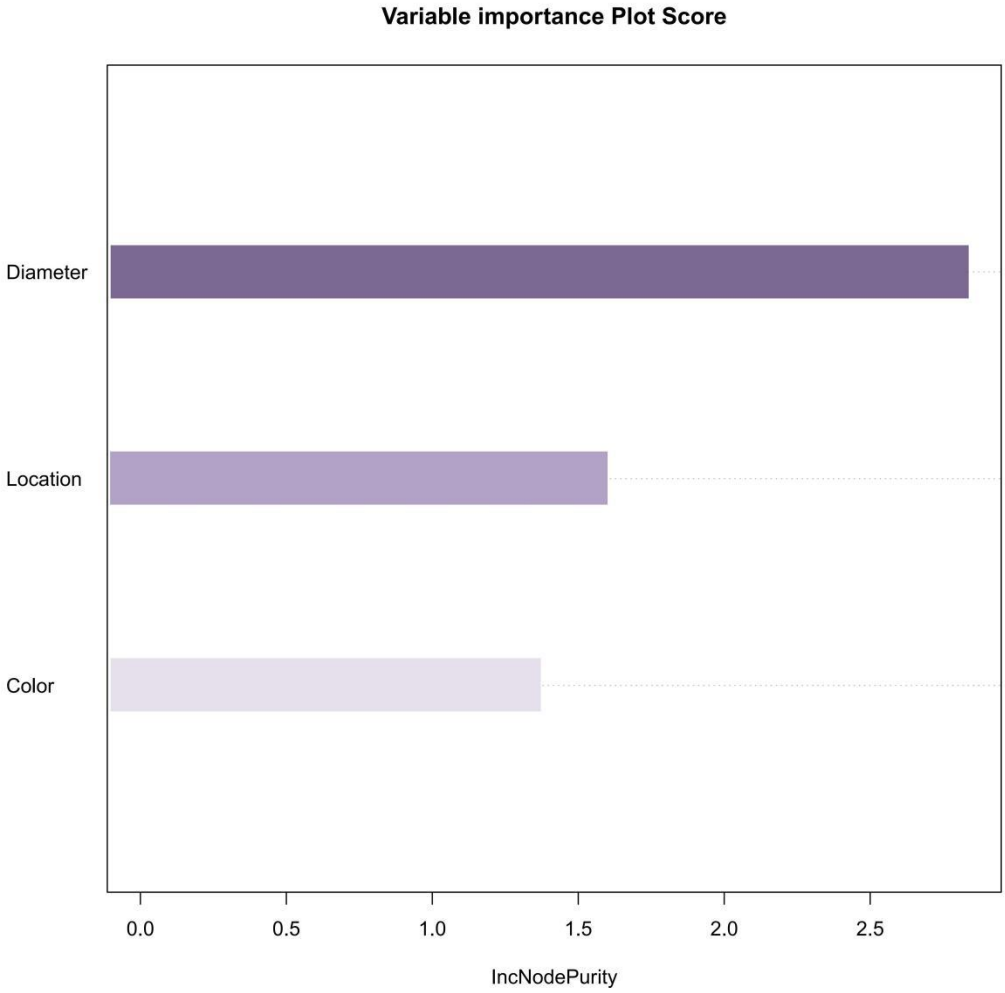

Figure 7. Feature importance ranks in random forest. The factors affecting the reliability of tumor area measurements, ranked in order of importance from highest to lowest, are diameter, color, and location.

5.3.3 Diameter

For tumors with a diameter >5 mm, the intra-rater and inter-rater ICC values were 0.976 (excellent) and 0.899 (good). The intra-rater and inter-rater REM were 7.80%(moderate) and 3.82% (very good), while the intra-rater and inter-rater MAD were 4.15 mm^3 and 2.15 mm^3, with TEM values exceeding 2 mm^3. The intra-rater and inter-rater rTEM were poor. For tumors with a diameter ≤5 mm, the intra-rater and inter-rater ICC (0.260 and 0.481) were poor, and both REM values were also poor. The intra- rater and inter-rater MAD were below 2 mm^3, but TEM values exceeded 2 mm^3 . Both intra-rater and inter-rater rTEM were poor. Compared to tumors 5 mm or smaller, tumors larger than 5 mm showed better overall measurement reliability (Figure 8 and Figure 9).

5.3.4 Color Characteristics

For red tumors, the intra-rater and inter-rater ICC (0.992 and 0.902) were excellent. The intra-rater MAD was 1.65 mm^3, while the inter-rater MAD was 3.81 mm^3. Regarding REM, the intra-rater REM was 5.71% (good), whereas the inter-rater REM was 12.07% (poor). Flesh-colored tumors showed good intra-rater ICC (0.831) but poor inter-rater ICC (0.482). The MAD values were 0.41 mm^3 for the intra-rater and 3.71 mm^3 for the inter-rater, with REM rated as very good for the intra-rater and poor for the inter-rater. Regarding yellow tumors, the intra-rater and inter-rater ICC were good (0.757) and moderate (0.747), respectively; the MAD values for intra-rater and inter-rater were greater than 2 mm^3, and the REM values were poor for both. As for brownish-black tumors, intra-rater and inter-rater ICC (0.990 and 0.989) were excellent; the MAD exceeded 2 mm^3, and the REM was moderate for intra-rater and poor for inter-rater measurements. The TEM for both intra-rater and inter-rater measurements of the four different periocular tumor colors were all greater than 2

mm³, and both rTEM were rated as poor. Overall, the volume measurement reliability was better for brown-black and red tumors, while yellow and flesh-colored tumors showed poorer reliability (Figure 8 and Figure 9).

5.3.5 Localization

In the upper eyelid, both intra-rater and inter-rater MAD values were below 2 mm³, with REM rated as very good for intra-rater (2.86%) and excellent for inter-rater (0.90%) measurements. In the lower eyelid, both intra-rater and inter-rater MAD values exceeded 2 mm³, with intra-rater REM rated as moderate (7.83%) and inter-rater REM rated as poor (15.44%). For tumors at the medial and lateral canthus, intra-rater MAD was below 2 mm³, while inter-rater MAD was above 2 mm³; REM was rated as excellent for intra-rater and poor for inter-rater measurements. The intra-rater rTEM at the lateral canthus was very good (2.66%), while rTEM was poor at other locations. Apart from the poor inter-rater ICC (0.381) at the medial canthus, all other locations had excellent ICC values for both intra-rater and inter-rater measurements. Except for the intra-rater TEM at the lateral canthus, which was below 2 mm³, TEM values for both intra-rater and inter-rater measurements at other locations were above 2 mm³.On the whole, the reliability of volume measurements was superior for the upper eyelid and lateral canthus compared to the lower eyelid and medial canthus (Figure 8 and Figure 9).

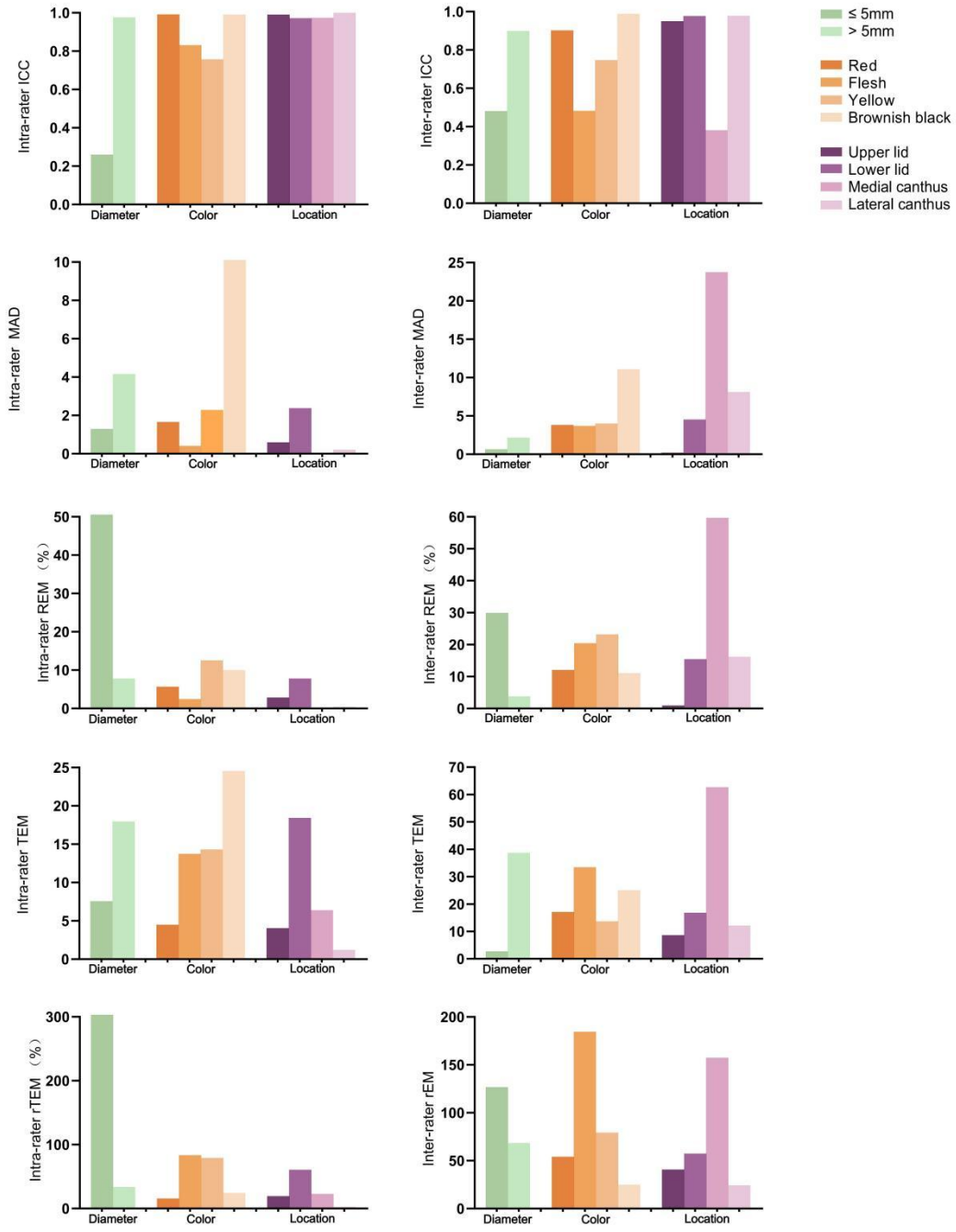

Figure 8. The bar graph shows the intra-and inter-rater reliability of tumor volume measurements, including intraclass correlation coefficient (ICC), mean absolute difference (MAD), technical error of measurement (TEM), relative error of measurement (REM), and relative TEM (rTEM).

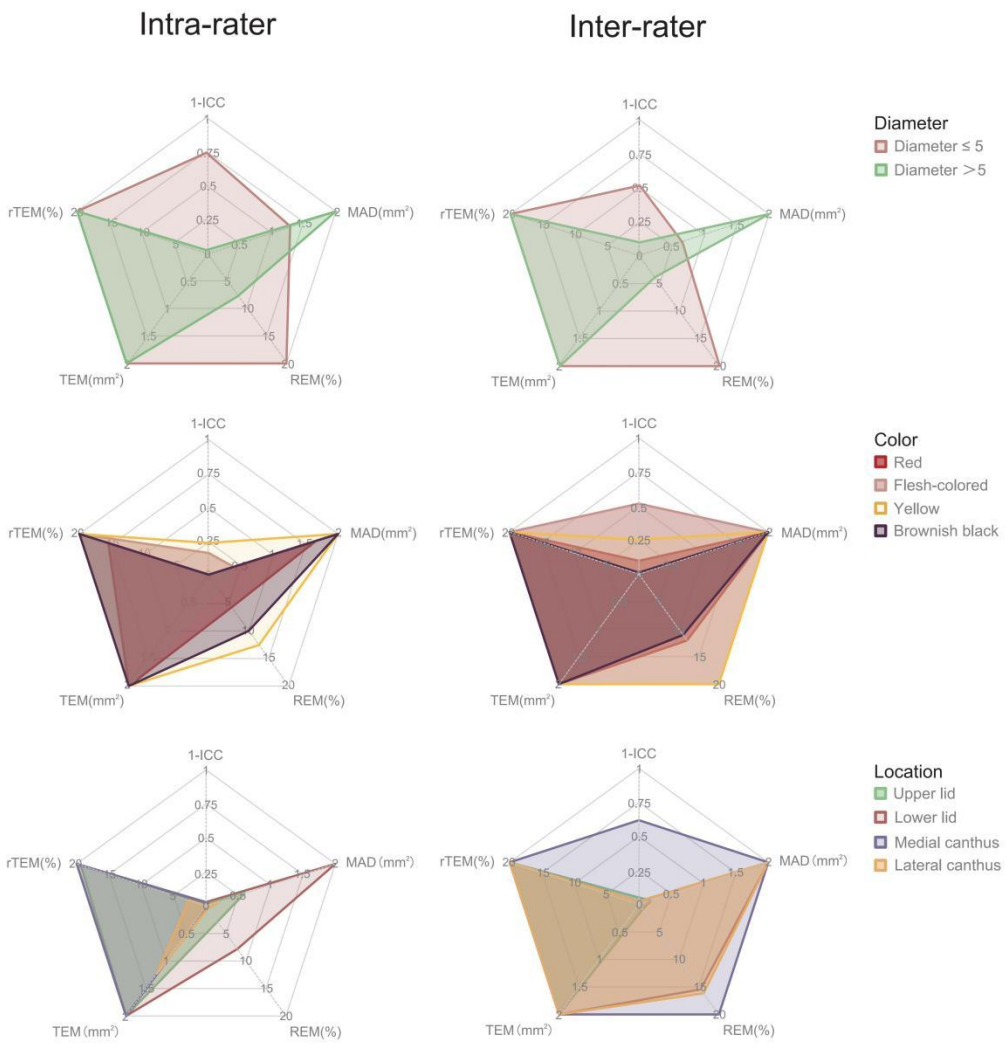

Figure 9. The radar graph offers a clearer visualization of the intra-rater and inter-rater reliability for different types of periocular tumor volume measurements, displaying the intraclass correlation coefficient (1-ICC), mean absolute difference (MAD), technical error of measurement (TEM), the relative error of measurement (REM), and relative TEM (rTEM). The smaller the area enclosed by the five different parameter points, the higher the reliability.

6. DISCUSSION

To our knowledge, this is the first study to measure the area and volume of periocular solid tumors directly and to evaluate intra-rater and inter-rater reliability. Before new technology can be widely applied in clinical practice, establishing its reliability is crucial to the validation process[60,61]. Previous studies have measured the area of the periocular region using idealized models[54]; however, actual tumors vary significantly in characteristics such as color, shape, and location. Therefore, conducting reliability studies on the actual tumor area is essential.

The study demonstrates that the overall reliability of periocular tumor area measurements is high, with MAD values remaining below two units. The intra-rater and inter-rater values for ICC, REM, TEM, and rTEM were 0.998 and 0.974, 1.94% and 1.22%, 2.29 mm² and 7.81 mm², and 6.95% and 23.76%, respectively. Except for the TEM and inter-rater rTEM, all other metrics indicated excellent or good reliability. Furthermore, the reliability of tumor volume measurements was generally lower compared to area measurements. While the intra-rater and inter-rater ICC were excellent, with MAD below two units and REM rated as good, however, both intra-rater and inter-rater TEM values exceeded two units, and rTEM was rated as poor. To further analyze the measurement reliability of tumors with different characteristics, we identified the factors that most significantly affect the reliability of tumor area and volume measurements from various variables. The selected factors for area measurements included tumor diameter, color, location, and boundary clarity, while the selected factors for volume measurements included tumor diameter, color, and location.

6.1 Diameter

The results of this study indicate that, for tumor area measurements, the reliability of measuring tumors larger than 5 mm is higher compared to those 5 mm or smaller, both within and between raters. Specifically, for tumors greater than 5 mm, the intra-rater reliability is rated as excellent or good, as indicated by the ICC (0.998), MAD (0.93 mm^2), REM (1.63%), TEM (2.43 mm^2), and rTEM (4.25%). Aside from TEM and rTEM, the inter-rater reliability is also high, with ICC, MAD, and REM values of 0.977, 0.85, and 1.52%, respectively. In terms of volume measurements, tumors with a diameter greater than 5 mm perform better on the ICC, REM, and rTEM metrics compared to those with a diameter of 5 mm or less. However, for MAD and TEM, tumors with a diameter of 5 mm or less show better measurements than those greater than 5 mm. This result is likely due to the fact that MAD and TEM are related to tumor size; smaller tumors result in lower MAD and TEM values. Overall, the reliability of measuring tumors with a diameter greater than 5 mm is slightly better than for those 5 mm or smaller.

The most common periocular skin cancers are BCC and squamous cell carcinoma SCC, both of which vary in tumor size, with larger tumors generally exhibiting higher aggressiveness[62,63]. For instance, known risk factors for BCC invasion of the orbit include large tumor size. Furthermore, the seventh edition of the American Joint Committee on Cancer (AJCC) staging manual includes a separate staging system for cutaneous squamous cell carcinoma, where a clinical size greater than 2 cm is a critical distinguishing factor, indicating high-risk features[64,65]. This study found that tumors larger than 5 mm exhibit excellent reliability, providing a robust basis for preoperative measurement of large, highly invasive malignant tumors and demonstrating significant potential for future applications.

6.2 Color Characteristics

In the area measurement of periocular tumors, comparing four tumor colors revealed that brownish-black tumors have the highest reliability, followed by flesh-colored and red tumors, while yellow tumors have the lowest reliability. However, the reliability observed in tumor volume measurements differed from those of area measurements. Our findings indicate that volume measurements for brown-black and red tumors are more reliable than those for flesh-colored and yellow tumors. Fan et al.obtained similar results using the same system. Their study involved printing 3D tumor models of various sizes and colors, placing them in different positions around the eye, measuring the tumor model volumes, and evaluating the intra-rater and inter-rater reliability of the measurements. The results indicated that the black tumor models exhibited good reliability [66]. Periocular melanoma is an aggressive tumor typically characterized by brown or tan pigmentation. Although relatively uncommon, comprising only 1% of eyelid tumors and melanomas, it has a high incidence of metastasis and mortality, with reports of a 10-year mortality rate approaching 30%[67]. Additionally, this malignancy is more prevalent among the elderly and female populations, with incidence rates increasing in recent years[6,68]. Combined with our results, it can be shown that stereophotogrammetry holds significant potential in accurately measuring the area and volume of eyelid melanomas. Merkel cell carcinoma (MCC) is another rare but highly aggressive malignancy, with most cases occurring in Caucasians and a much lower incidence observed in other races[69]. MCC carries a high risk of metastasis and recurrence[70,71]. Lesions typically present as solitary purple or red nodules on the eyelid margin, often resulting in partial or complete loss of eyelashes[69,72]. Basal cell carcinoma (BCC) accounts for 90% of malignant eyelid tumors and is the most common malignancy in the periocular region[73].It develops slowly, with the classic presentation being a pearly nodule, most

often appearing as a solitary flesh-colored lesion[74]. Squamous cell carcinoma (SCC) is the second most common malignancy in the periocular region[75], and it can present in various forms, including erythematous scaly plaques or raised flesh-colored plaques and nodules[6,76]. Our study indicates that the stereophotogrammetry system demonstrates high reliability in measuring the surface area of flesh-colored and red tumors, suggesting significant potential for its application in measuring BCC, SCC, and MCC tumors in the future. Regarding volume, the stereophotogrammetry system demonstrates high reliability in measuring the surface area of brown-black and red tumors. Therefore, using stereoscopic imaging devices for volume measurements of red SCCs, MCCs, and eyelid melanoma offers relatively good reliability.These findings suggest that stereophotogrammetry provides a promising approach for evaluating tumor areas and volumes, enhancing the reliability of measurements for these specific tumor types and aiding in clinical assessment and management.

6.3 Localization

The reliability of periocular tumor measurements varies according to their location. Our study suggested that tumors in the medial canthus exhibited the lowest measurement reliability, consistent with the findings of Liu et al., who also identified the medial canthus as having the poorest reliability in their study on periocular region area reliability[54]. This may be attributed to the difficulty in fully exposing tumors in the medial canthus, where the nasal bridge can interfere, resulting in image artifacts that compromise measurement accuracy. In the measurement of tumor volume, we found that the reliability was higher for tumors located at the lateral canthus and upper eyelid, while it was lower for those at the medial canthus and upper eyelid. This finding is similar to the results reported by Fan et al. on the reliability of periocular tumor model volume measurements, which showed good reliability when the tumors

were at the upper eyelid and lateral canthus[66]. However, unlike our results, their study also found good reliability at the medial canthus. This discrepancy may be because our study involved real periocular tumors in patients, whereas their research was based on tumor models. Tumors in patient eyelids tend to exhibit more complexity and are less uniform, which may account for the observed differences in the findings. The lower eyelid is the most frequent location for periocular BCC, accounting for approximately 50-60% of cases[77]. Similarly, SCC, another common non-melanoma skin cancer, predominantly occurs in the lower eyelid, with 48%–68% of cases[16]. Both types of tumors are associated with ultraviolet radiation exposure, and their higher prevalence in the lower eyelid is because the lower eyelids are more directly exposed to sunlight[78]. Sebaceous gland carcinoma (SGC), a rare malignancy that is more prevalent among Asians, frequently affects the upper eyelid due to the higher density of meibomian glands and typically presents as a painless subcutaneous nodule[29,65]. BCC and SCC may also arise on the lateral eyelid; however, these occurrences are less frequent than tumors at the eyelid margin and present a higher propensity for orbital invasion [79,80]. Our study found that in terms of tumor area measurement, tumors located at the lateral canthus, lower eyelid, and upper eyelid exhibited higher measurement reliability. For volume measurement, tumors at the lateral canthus and upper eyelid showed good reliability. The results indicating that this method offers a more accurate and convenient approach for assessing tumors in commonly affected areas for BCC and SCC, as well as for highly aggressive tumors.

6.4 Boundary

Our study found better reliability for well-defined tumors than for ill-defined tumors in area measurements. Notably, inter-rater reliability exhibited greater variability compared to intra-rater reliability, likely due to discrepancies in boundary identification

by different raters for tumors with indistinct margins, leading to intergroup differences in measurement outcomes. Clinically, benign tumors typically present with distinct boundaries, whereas malignant tumors often manifest with ambiguous margins[81]. Consequently, for more accurate and reliable measurements in clinical settings, it is advisable that tumors with poorly defined margins be identified collaboratively by several experienced doctors. This approach is expected to improve the consistency and reliability of the measurements.

It is noteworthy that in our study,the REM and rTEM values for many tumors were relatively high. This observation may be attributed to the relatively small size of periorbital tumors, as tumors with smaller areas tend to have higher REM and rTEM values. This finding is consistent with previous research, which shows that larger objects have higher MAD and TEM values, while REM and rTEM values decrease with increasing area. Conversely, smaller objects exhibit lower MAD and TEM values but higher REM and rTEM values[51,82].

This study represents the first comprehensive analysis involving precise measurement of periocular tumor areas and volume, compiling reliable data on the measurement accuracy for tumors in the periocular region. These findings hold significant value for the clinical assessment of periocular tumors. For instance, surgical intervention remains the preferred treatment modality for periocular tumors such as BCC and SCC. The size of a tumor holds significant importance in assessing the extent of preoperative skin excision, selecting the most appropriate surgical approach, and evaluating prognosis, which is crucial for the postoperative functional and aesthetic recovery of the patient's eyelids. Traditionally, clinical assessment has primarily relied on measuring the tumor diameter, which provides a limited evaluation

criterion. Integrating tumor area and volume measurements into preoperative assessments could substantially enhance accuracy. Moreover, eyelid tumors, particularly prevalent malignant types such as BCC and SCC, exhibit slow growth and insidious progression[9]. Given the constraints of periocular anatomy, subtle changes in tumor size are challenging to discern visually. In such cases, using stereophotogrammetry for patient follow-up makes it easier to detect changes in tumor size, allowing for better planning of subsequent treatment strategies.

This research also has several limitations. Despite the large sample size, the number of cases within different subcategories of characteristics is not evenly distributed. For example, the smaller number of brownish-black and yellow tumors may either increase or decrease the reliability of findings related to these subgroups. Further research is needed to confirm these trends in a larger sample and ensure an equitable distribution of cases across different groups, allowing for consistent assessment of the outcomes. Moreover, as periocular tumors, particularly malignant ones, are more prevalent in elderly individuals, this study predominantly included older participants. Considering the anatomical differences between younger and older patients, further research is needed to determine if these findings apply to younger populations. Future studies could investigate larger and more diverse patient cohorts to enhance the robustness and applicability of the findings.

Our study established the feasibility of measuring the area and volume of periorbital tumors and confirmed the high reliability of using 3D stereophotogrammetry for these measurements, particularly in measuring tumor area. Tumors larger than 5 mm, characterized by a brownish-black color, clear boundaries, and located at the lateral canthus, upper eyelid, or lower eyelid, demonstrated higher reliability in area

measurements. For volume measurements, tumors larger than 5 mm, with a brownish-black or red color, and located at the lateral canthus or upper eyelid exhibited high reliability. These findings highlight the potential for 3D stereophotogrammetry to improve surgical planning, especially for larger periocular tumors or those with specific characteristics. By providing accurate and reproducible measurements, this technology could help guide excision strategies, optimize margin assessment, and potentially reduce recurrence rates, ultimately enhancing patient outcomes. Looking ahead, this measurement approach holds promise for expanding beyond periocular tumors to other anatomical regions or tumor types. Its application in broader clinical settings could further validate its utility, offering a reliable, non-invasive tool for tumor measurement and treatment planning across various fields of oncology.

7. REFERENCES

1. Bernardini FP. Management of malignant and benign eyelid lesions. *Curr Opin Ophthalmol* 2006; **17**(5): 480-4.
2. Varde MA, Heindl LM, Kakkassery V. [Diagnosis and treatment of benign eyelid tumors]. *Ophthalmologie* 2023; **120**(3): 240-51.
3. Sendul SY, Akpolat C, Yilmaz Z, Eryilmaz OT, Guven D, Kabukcuoglu F. Clinical and pathological diagnosis and comparison of benign and malignant eyelid tumors. *J Fr Ophtalmol* 2021; **44**(4): 537-43.
4. Deprez M, Uffer S. Clinicopathological features of eyelid skin tumors. A retrospective study of 5504 cases and review of literature. *Am J Dermatopathol* 2009; **31**(3): 256-62.
5. Xu XL, Li B, Sun XL, et al. Eyelid neoplasms in the Beijing Tongren Eye Centre between 1997 and 2006. *Ophthalmic Surg Lasers Imaging* 2008; **39**(5): 367-72.
6. Moran JM, Phelps PO. Periocular skin cancer: Diagnosis and management. *Dis Mon* 2020; **66**(10): 101046.
7. Yin VT, Merritt HA, Sniegowski M, Esmaeli B. Eyelid and ocular surface carcinoma: diagnosis and management. *Clin Dermatol* 2015; **33**(2): 159-69.
8. Cook BE, Jr., Bartley GB. Epidemiologic characteristics and clinical course of patients with malignant eyelid tumors in an incidence cohort in Olmsted County, Minnesota. *Ophthalmology* 1999; **106**(4): 746-50.
9. Silverman N, Shinder R. What's New in Eyelid Tumors. *Asia Pac J Ophthalmol (Phila)* 2017; **6**(2): 143-52.
10. Shi Y, Jia R, Fan X. Ocular basal cell carcinoma: a brief literature review of clinical diagnosis and treatment. *Onco Targets Ther* 2017; **10**: 2483-9.
11. Wojno TH. The association between cigarette smoking and basal cell carcinoma of the eyelids in women. *Ophthalmic Plast Reconstr Surg* 1999; **15**(6): 390-2.
12. Nemet AY, Deckel Y, Martin PA, et al. Management of periocular basal and squamous cell carcinoma: a series of 485 cases. *Am J Ophthalmol* 2006; **142**(2): 293-7.
13. Malhotra R, Huilgol SC, Huynh NT, Selva D. The Australian Mohs database, part II: periocular basal cell carcinoma outcome at 5-year follow-up. *Ophthalmology* 2004; **111**(4): 631-6.
14. Echchaoui A, Benyachou M, Houssa A, et al. [Management of eyelid carcinomas: Retrospective bicentric study of 64 cases and review of the literature]. *J Fr Ophtalmol* 2016; **39**(2): 187-94.
15. Thosani MK, Schneck G, Jones EC. Periocular squamous cell carcinoma. *Dermatol Surg* 2008; **34**(5): 585-99.
16. Limawararut V, Leibovitch I, Sullivan T, Selva D. Periocular squamous cell carcinoma. *Clin Exp Ophthalmol* 2007; **35**(2): 174-85.
17. Leibovitch I, Huilgol SC, Selva D, Hill D, Richards S, Paver R. Cutaneous squamous cell carcinoma treated with Mohs micrographic surgery in Australia I. Experience over 10 years. *J Am Acad Dermatol* 2005; **53**(2): 253-60.

18. Petter G, Haustein UF. Histologic subtyping and malignancy assessment of cutaneous squamous cell carcinoma. *Dermatol Surg* 2000; **26**(6): 521-30.
19. Tong JY, Huilgol SC, James C, Rajak S, Selva D. Perineural invasion and perineural spread in periocular squamous cell carcinoma. *Eye (Lond)* 2023; **37**(5): 875-84.
20. Cook BE, Jr., Bartley GB. Treatment options and future prospects for the management of eyelid malignancies: an evidence-based update. *Ophthalmology* 2001; **108**(11): 2088-98; quiz 99-100, 121.
21. Donaldson MJ, Sullivan TJ, Whitehead KJ, Williamson RM. Squamous cell carcinoma of the eyelids. *Br J Ophthalmol* 2002; **86**(10): 1161-5.
22. Boulos PR, Rubin PA. Cutaneous melanomas of the eyelid. *Semin Ophthalmol* 2006; **21**(3): 195-206.
23. Bunnell AM, Nedrud SM, Fernandes RP. Classification and Staging of Melanoma in the Head and Neck. *Oral Maxillofac Surg Clin North Am* 2022; **34**(2): 221-34.
24. Freitag SK, Aakalu VK, Tao JP, et al. Sentinel Lymph Node Biopsy for Eyelid and Conjunctival Malignancy: A Report by the American Academy of Ophthalmology. *Ophthalmology* 2020; **127**(12): 1757-65.
25. Dores GM, Curtis RE, Toro JR, Devesa SS, Fraumeni JF, Jr. Incidence of cutaneous sebaceous carcinoma and risk of associated neoplasms: insight into Muir-Torre syndrome. *Cancer* 2008; **113**(12): 3372-81.
26. Kaliki S, Bothra N, Bejjanki KM, et al. Malignant Eyelid Tumors in India: A Study of 536 Asian Indian Patients. *Ocul Oncol Pathol* 2019; **5**(3): 210-9.
27. Muqit MM, Foot B, Walters SJ, Mudhar HS, Roberts F, Rennie IG. Observational prospective cohort study of patients with newly-diagnosed ocular sebaceous carcinoma. *Br J Ophthalmol* 2013; **97**(1): 47-51.
28. Kass LG, Hornblass A. Sebaceous carcinoma of the ocular adnexa. *Surv Ophthalmol* 1989; **33**(6): 477-90.
29. Song A, Carter KD, Syed NA, Song J, Nerad JA. Sebaceous cell carcinoma of the ocular adnexa: clinical presentations, histopathology, and outcomes. *Ophthalmic Plast Reconstr Surg* 2008; **24**(3): 194-200.
30. Husain A, Blumenschein G, Esmaeli B. Treatment and outcomes for metastatic sebaceous cell carcinoma of the eyelid. *Int J Dermatol* 2008; **47**(3): 276-9.
31. Heath M, Jaimes N, Lemos B, et al. Clinical characteristics of Merkel cell carcinoma at diagnosis in 195 patients: the AEIOU features. *J Am Acad Dermatol* 2008; **58**(3): 375-81.
32. Peters GB, 3rd, Meyer DR, Shields JA, et al. Management and prognosis of Merkel cell carcinoma of the eyelid. *Ophthalmology* 2001; **108**(9): 1575-9.
33. Gupta SG, Wang LC, Peñas PF, Gellenthin M, Lee SJ, Nghiem P. Sentinel lymph node biopsy for evaluation and treatment of patients with Merkel cell carcinoma: The Dana-Farber experience and meta-analysis of the literature. *Arch Dermatol* 2006; **142**(6): 685-90.
34. Assouline A, Tai P, Joseph K, Lian JD, Krzisch C, Yu E. Merkel cell carcinoma of skin-current controversies and recommendations. *Rare Tumors* 2011; **3**(2): e23.

35. Yamamoto S, Miyachi H, Fujii H, Ochiai S, Watanabe S, Shimozato K. Intuitive Facial Imaging Method for Evaluation of Postoperative Swelling: A Combination of 3-Dimensional Computed Tomography and Laser Surface Scanning in Orthognathic Surgery. *J Oral Maxillofac Surg* 2016; **74**(12): 2506.e1-.e10.
36. Knoops PG, Beaumont CA, Borghi A, et al. Comparison of three-dimensional scanner systems for craniomaxillofacial imaging. *J Plast Reconstr Aesthet Surg* 2017; **70**(4): 441-9.
37. Gibelli D, Pucciarelli V, Cappella A, Dolci C, Sforza C. Are Portable Stereophotogrammetric Devices Reliable in Facial Imaging? A Validation Study of VECTRA H1 Device. *J Oral Maxillofac Surg* 2018; **76**(8): 1772-84.
38. Ferrario VF, Sforza C, Poggio CE, Cova M, Tartaglia G. Preliminary evaluation of an electromagnetic three-dimensional digitizer in facial anthropometry. *Cleft Palate Craniofac J* 1998; **35**(1): 9-15.
39. Jones PR, West GM, Harris DH, Read JB. The Loughborough anthropometric shadow scanner (LASS). *Endeavour* 1989; **13**(4): 162-8.
40. Hajeer MY, Millett DT, Ayoub AF, Siebert JP. Applications of 3D imaging in orthodontics: part I. *J Orthod* 2004; **31**(1): 62-70.
41. Al-Omari I, Millett DT, Ayoub AF. Methods of assessment of cleft-related facial deformity: a review. *Cleft Palate Craniofac J* 2005; **42**(2): 145-56.
42. Heike CL, Upson K, Stuhaug E, Weinberg SM. 3D digital stereophotogrammetry: a practical guide to facial image acquisition. *Head Face Med* 2010; **6**: 18.
43. Weinberg SM, Kolar JC. Three-dimensional surface imaging: limitations and considerations from the anthropometric perspective. *J Craniofac Surg* 2005; **16**(5): 847-51.
44. Yang Y, Xia Z, Shi Y, et al. A Quantitative Three-Dimensional Tear Trough Deformity Assessment and Its Application in Orbital Septum Fat Transposition. *Aesthetic Plast Surg* 2023; **47**(6): 2453-60.
45. Ayaz I, Shaheen E, Aly M, et al. Accuracy and reliability of 2-dimensional photography versus 3-dimensional soft tissue imaging. *Imaging Sci Dent* 2020; **50**(1): 15-22.
46. Yang Y, Zhang M, Jin L, et al. Gender- and Age-Related Characterization of Lip Morphology: A Three-Dimensional Analysis in a Chinese Population. *Aesthet Surg J* 2023; **43**(12): Np990-np1000.
47. Sowmya MV, Mehrotra D, Mohammad S, et al. 3D assessment of ear morphology. *J Oral Biol Craniofac Res* 2023; **13**(5): 622-9.
48. Chen G, Hsieh EY, Chen SH, et al. Occlusion-Based Three-Dimensional Craniofacial Anthropometric and Symmetric Evaluation in Preadolescences: A Comparative COHORT Study. *J Clin Med* 2023; **12**(15).
49. Dallazen E, Baccaro GC, Santos AMS, et al. Comparison of Manual (2D) and Digital (3D) Methods in the Assessment of Simulated Facial Edema. *J Oral Maxillofac Surg* 2023; **81**(9): 1146-54.
50. Andrews J, Alwafi A, Bichu YM, Pliska BT, Mostafa N, Zou B. Validation of three-dimensional facial imaging captured with smartphone-based photogrammetry

application in comparison to stereophotogrammetry system. *Heliyon* 2023; **9**(5): e15834.
51. Guo Y, Hou X, Rokohl AC, Jia R, Heindl LM. Reliability of Periocular Anthropometry: A Comparison of Direct, 2-Dimensional, and 3-Dimensional Techniques. *Dermatol Surg* 2020; **46**(9): e23-e31.
52. De Stefani A, Barone M, Hatami Alamdari S, et al. Validation of Vectra 3D Imaging Systems: A Review. *Int J Environ Res Public Health* 2022; **19**(14).
53. Fan W, Guo Y, Hou X, et al. Validation of the Portable Next-Generation VECTRA H2 3D Imaging System for Periocular Anthropometry. *Front Med (Lausanne)* 2022; **9**: 833487.
54. Liu J, Rokohl AC, Guo Y, et al. Reliability of Stereophotogrammetry for Area Measurement in the Periocular Region. *Aesthetic Plast Surg* 2021; **45**(4): 1601-10.
55. Koo TK, Li MY. A Guideline of Selecting and Reporting Intraclass Correlation Coefficients for Reliability Research. *J Chiropr Med* 2016; **15**(2): 155-63.
56. Dindaroğlu F, Kutlu P, Duran GS, Görgülü S, Aslan E. Accuracy and reliability of 3D stereophotogrammetry: A comparison to direct anthropometry and 2D photogrammetry. *Angle Orthod* 2016; **86**(3): 487-94.
57. Guo Y, Rokohl AC, Schaub F, et al. Reliability of periocular anthropometry using three-dimensional digital stereophotogrammetry. *Graefes Arch Clin Exp Ophthalmol* 2019; **257**(11): 2517-31.
58. Verhulst A, Hol M, Vreeken R, Becking A, Ulrich D, Maal T. Three-Dimensional Imaging of the Face: A Comparison Between Three Different Imaging Modalities. *Aesthet Surg J* 2018; **38**(6): 579-85.
59. Ulijaszek SJ, Kerr DA. Anthropometric measurement error and the assessment of nutritional status. *Br J Nutr* 1999; **82**(3): 165-77.
60. Lübbers HT, Medinger L, Kruse AL, Grätz KW, Obwegeser JA, Matthews F. The influence of involuntary facial movements on craniofacial anthropometry: a survey using a three-dimensional photographic system. *Br J Oral Maxillofac Surg* 2012; **50**(2): 171-5.
61. Luebbers HT, Messmer P, Obwegeser JA, et al. Comparison of different registration methods for surgical navigation in cranio-maxillofacial surgery. *J Craniomaxillofac Surg* 2008; **36**(2): 109-16.
62. Sun MT, Wu A, Figueira E, Huilgol S, Selva D. Management of periorbital basal cell carcinoma with orbital invasion. *Future Oncol* 2015; **11**(22): 3003-10.
63. Walling HW, Fosko SW, Geraminejad PA, Whitaker DC, Arpey CJ. Aggressive basal cell carcinoma: presentation, pathogenesis, and management. *Cancer Metastasis Rev* 2004; **23**(3-4): 389-402.
64. Farasat S, Yu SS, Neel VA, et al. A new American Joint Committee on Cancer staging system for cutaneous squamous cell carcinoma: creation and rationale for inclusion of tumor (T) characteristics. *J Am Acad Dermatol* 2011; **64**(6): 1051-9.
65. Slutsky JB, Jones EC. Periocular cutaneous malignancies: a review of the literature. *Dermatol Surg* 2012; **38**(4): 552-69.

66. Fan W, Rokohl AC, Kupka P, et al. Reproducibility of Three-Dimensional Volumetric Measurement of Periocular Tumor Models. *Ophthalmol Ther* 2023; **12**(1): 111-23.
67. Oliver JD, Boczar D, Sisti A, et al. Eyelid Melanoma in the United States: A National Cancer Database Analysis. *J Craniofac Surg* 2019; **30**(8): 2412-5.
68. Sitenga JL, Aird G, Ahmed A, Walters R, Silberstein PT. Socioeconomic status and survival for patients with melanoma in the United States: an NCDB analysis. *Int J Dermatol* 2018; **57**(10): 1149-56.
69. Herbert HM, Sun MT, Selva D, et al. Merkel cell carcinoma of the eyelid: management and prognosis. *JAMA Ophthalmol* 2014; **132**(2): 197-204.
70. Lemos BD, Storer BE, Iyer JG, et al. Pathologic nodal evaluation improves prognostic accuracy in Merkel cell carcinoma: analysis of 5823 cases as the basis of the first consensus staging system. *J Am Acad Dermatol* 2010; **63**(5): 751-61.
71. Smith VA, Camp ER, Lentsch EJ. Merkel cell carcinoma: identification of prognostic factors unique to tumors located in the head and neck based on analysis of SEER data. *Laryngoscope* 2012; **122**(6): 1283-90.
72. Merritt H, Sniegowski MC, Esmaeli B. Merkel cell carcinoma of the eyelid and periocular region. *Cancers (Basel)* 2014; **6**(2): 1128-37.
73. Saleh GM, Desai P, Collin JR, Ives A, Jones T, Hussain B. Incidence of eyelid basal cell carcinoma in England: 2000-2010. *Br J Ophthalmol* 2017; **101**(2): 209-12.
74. Pe'er J. Pathology of eyelid tumors. *Indian J Ophthalmol* 2016; **64**(3): 177-90.
75. Sullivan TJ. Squamous cell carcinoma of eyelid, periocular, and periorbital skin. *Int Ophthalmol Clin* 2009; **49**(4): 17-24.
76. Mukarram M, Khachemoune A. Upper and Lower Eyelid Malignancies: Differences in Clinical Presentation, Metastasis, and Treatment. *Arch Dermatol Res* 2024; **316**(7): 429.
77. Totir M, Alexandrescu C, Pirvulescu R, Gradinaru S, Costache M. Clinical, Histopathological and Therapeutical Analysis of Inferior Eyelid Basal Cell Carcinomas. *J Med Life* 2014; **7 Spec No. 4**(Spec Iss 4): 18-22.
78. Furdova A, Kapitanova K, Kollarova A, Sekac J. Periocular basal cell carcinoma - clinical perspectives. *Oncol Rev* 2020; **14**(1): 420.
79. Selva D, Hale L, Bouskill K, Huilgol SC. Recurrent morphoeic basal cell carcinoma at the lateral canthus with orbitocranial invasion. *Australas J Dermatol* 2003; **44**(2): 126-8.
80. Monheit G, Hrynewycz K. Mohs Surgery for Periocular Tumors. *Dermatol Surg* 2019; **45 Suppl 2**: S70-s8.
81. Montemezzi S, Peroni A, Nigro M, Saggin P, Tinazzi Martini P, Gortenuti G. [Echographic assessment of cutaneous neoplasms]. *Radiol Med* 1993; **85**(5 Suppl 1): 156-61.
82. Andrade LM, Rodrigues da Silva AMB, Magri LV, Rodrigues da Silva MAM. Repeatability Study of Angular and Linear Measurements on Facial Morphology Analysis by Means of Stereophotogrammetry. *J Craniofac Surg* 2017; **28**(4): 1107-11.

8. APPENDIX

8.1 Figure legends

Figure 1. VECTRA M3 dimension and Patients with Periocular Tumors Captured Using the VECTRA M3 Imaging System.

Figure 2. LASSO regression combined with 10-fold cross-validation.

Figure 3. Feature importance ranks in random forest.

Figure 4. Bar Graph of intra- and inter-rater reliability in tumor area measurements.

Figure 5. Radar graph of intra- and inter-rater reliability in periocular tumor area measurements.

Figure 6. LASSO regression combined with 10-fold cross-validation.

Figure 7. Feature importance ranks in random forest.

Figure 8. Bar Graph of intra- and inter-rater reliability in tumor volume measurements.

Figure 9. Radar graph of intra- and inter-rater reliability in periocular tumor volume measurements.

8.2 Table legend

Table 1 The demographic and clinical features of patients with eyelid tumors

9. PUBLICATIONS

1.**Hou X**, Rokohl AC, Berndt K, Li S, Ju X, Matos PAW, Fan W, Heindl LM. Risk factors analysis and nomogram for predicting recurrence in periocular basal cell carcinoma. Can J Ophthalmol. 2024 Dec 30:S0008-4182(24)00368-5. doi: 10.1016/j.jcjo.2024.12.003. Epub ahead of print. PMID: 39746661.

2.**Hou X**, Rokohl AC, Li X, Guo Y, Ju X, Fan W, Heindl LM. Global incidence and prevalence in uveal melanoma. Adv Ophthalmol Pract Res. 2024 Oct 9;4(4):226-232. doi: 10.1016/j.aopr.2024.10.001. PMID: 39726825; PMCID:PMC11670701.

3.**Hou X**, Rokohl AC, Fan W, Guo Y, Ali MJ, Heindl LM. Periocular Malignancies and Postoperative Eyelid Reconstruction. Int Ophthalmol Clin. 2023;63(3):147-162.